Macromolecules **1991,** *24,* 1017-1024

Molecular Engineering of Liquid-Crystal Polymers by Living Polymerization. 3.[†] Influence of Molecular Weight on the Phase Transitions of Poly{8-[(4-cyano-4′-biphenyl)oxy]octyl vinyl ether} and of Poly{6-[(4-cyano-4′-biphenyl)oxy]hexyl vinyl ether}

V. Percec* and M. Lee

Department of Macromolecular Science, Case Western Reserve University, Cleveland, Ohio 44106

Received April 11, 1990; Revised Manuscript Received August 17, 1990

ABSTRACT: The synthesis and living cationic polymerization of 8-[(4-cyano-4′-biphenyl)oxy]octyl vinyl ether (6–8) and of 6-[(4-cyano-4′-biphenyl)oxy]hexyl vinyl ether (6-6) are described. The mesomorphic behavior of poly(6-8) and poly(6-6) with different degrees of polymerization and narrow molecular weight distribution was compared to that of the 6-8 and 6-6 and of 8-[(4-cyano-4′-biphenyl)oxy]octyl ethyl ether (8-8) and 6-[(4-cyano-4′-biphenyl)oxy]hexyl ethyl ether (8-6). 8-8 and 8-6 are the model compounds of the monomeric structural units of poly(6-8) and poly(6-6). 6-8 displays an enantiotropic nematic mesophase, 6-6 and 8-6 exhibit a monotropic nematic mesophase, and 8-8 gives a monotropic nematic and a monotropic s_A mesophase. Poly(6-8) with a degree of polymerization of 2.1 and poly(6-6)s with degrees of polymerization from 3.3 to 7.3 display an enantiotropic s_A and an enantiotropic nematic mesophase. Poly(6-8)s with degrees of polymerization from 4.2 to 10.2 and poly(6-6)s with degrees of polymerization from 7.6 to 13.5 display an enantiotropic s_A mesophase. Poly(6-8)s with degrees of polymerization larger than 12.4 and poly(6-6)s with degrees of polymerization higher than 23.2 display an enantiotropic s_X (i.e., an unidentified smectic phase) and an enantiotropic s_A mesophase. Poly(6-8)s and poly(6-6)s with degrees of polymerization from 1 (i.e., 8-8 and 8-6) to 30.0 represent the first examples of side-chain liquid-crystalline polymers that show a continuous change of the mesomorphic–isotropic phase transition (i.e., from nematic–isotropic to smectic–isotropic) on increasing their molecular weight.

Introduction

The most elementary step toward the molecular design of side-chain liquid-crystalline polymers represents the elucidation of the mechanism by which the polymer molecular weight influences its phase behavior. So far, the only trend that is generally accepted consists of the enlargement of the temperature range of the mesophase with an increase of the polymer molecular weight.[1-14] This dependence was recently explained on the basis of thermodynamic principles assuming that the phase behavior of the polymer is determined by that of the monomeric structural unit.[12,13] So far there are two experiments in the literature in which the phase behavior of a polymer with different molecular weights was compared to that of the model compound of its monomeric structural unit.[7,11] In both cases the model compound of the monomeric structural unit and the polymers with different molecular weights display the same type of mesophase. A second mesophase may however appear above a certain polymer molecular weight.[7,11] This trend can be easily explained on the basis of thermodynamics.[12,13] There are additional examples in the literature where a polymer displays various mesophases at different molecular weights.[4,9,10] However, no information is available on the phase behavior of the models of their monomeric structural units. Elucidation of this phenomenon requires the synthesis and characterization of polymers with well-defined molecular weights and narrow molecular weight distributions as well as of the model compounds of their monomeric structural units. So far, side-chain liquid-crystalline polymers with narrow molecular weight distribution were prepared by group-transfer polymerization of mesogenic methacrylates,[7] by cationic polymerization of mesogenic vinyl and propenyl ethers,[8-11,14,15] and by polymer homologous reactions.[16]

Scheme I
Synthesis of Monomers and Model Compounds

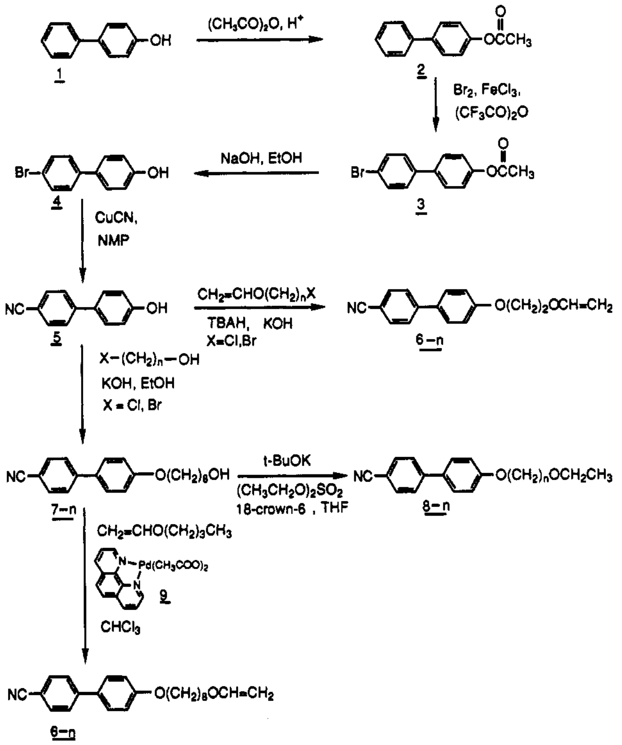

This paper will present the synthesis and living cationic polymerization of 8-[(4-(cyano-4′-biphenyl)oxy]octyl vinyl ether (6-8) and 6-[(4-cyano-4′-biphenyl)oxy]hexyl vinyl ether (6-6) and the mesomorphic behavior of the resulting polymers with different molecular weights. The phase behavior of these polymers will be compared to that of 8-[(4-cyano-4′-biphenyl)oxy]octyl ethyl ether (8-8) and 6-[(4-cyano-4′-biphenyl)oxy]hexyl ethyl ether (8-6), which

[†] Part 2 of this series: ref 11.

0024-9297/91/2224-1017$02.50/0

Table I
Thermal Characterization of 4-Cyano-4′-(8-hydroxyoctan-1-yloxy)biphenyl (7–8), 4-Cyano-4′-(6-hydroxyhexan-1-yloxy)biphenyl (7–6), 8-[(4-Cyano-4′-biphenyl)oxy]octyl Vinyl Ether (6–8), 6-[(4-Cyano-4′-biphenyl)oxy]hexyl Vinyl Ether (6–6), 8-[(4-Cyano-4′-biphenyl)oxy]octyl Ethyl Ether (8–8), and 6-[(4-Cyano-4′-biphenyl)oxy]hexyl Ethyl Ether (8–6)[a]

	phase transitions, 0 °C (corresponding enthalpy changes, kcal/mru)	
compd	heating	cooling
7–8	k 87.7 (9.1) n 104.0 (0.23) i	i 100.4 (0.38) n 57.7 (6.09) k
7–6	k 93.5 (8.01) 110.9 (0.25) i	i 107.8 (0.33) n 71.04 (5.66) k
6–8	k 54.0 (8.31) n 70.8 (0.27) i	i 67.3 (0.31) n 27.9 (4.68) k
6–6	k 75.5 (5.95) [n 75.9 (0.35)] i	i 68.2 (0.31) n 55.8 (5.22) k
8–8	k 62.9 (8.77) [s_A 58.5 (0.26) n 61.0 (0.39)] i	i 53.1 (0.37) n 46.9 (0.015) s_A 23.7 (7.21) k
8–6	k 64.6 (8.67) [n 60.0 (0.12)] i	i 46.7 (0.13) n 27.1 (7.21) k

[a] Values in brackets represent virtual data.

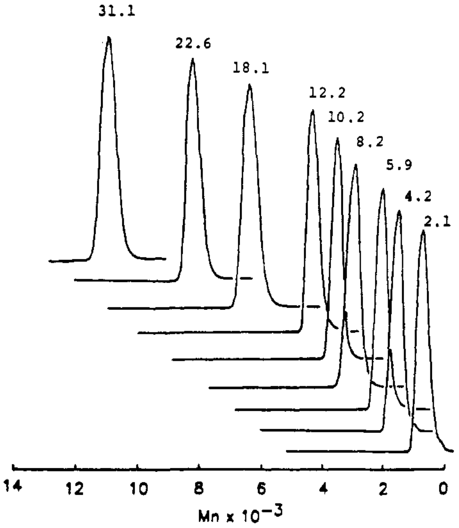

Figure 1. GPC traces of poly(6-8). The degree of polymerization of each sample is printed on the figure.

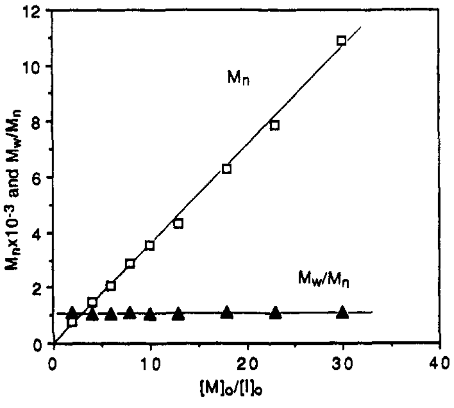

Figure 2. Dependence of the number average molecular weight (M_n) and of the polydispersity (M_w/M_n) of poly(6-8) on the $[M]_0/[I]_0$ ratio.

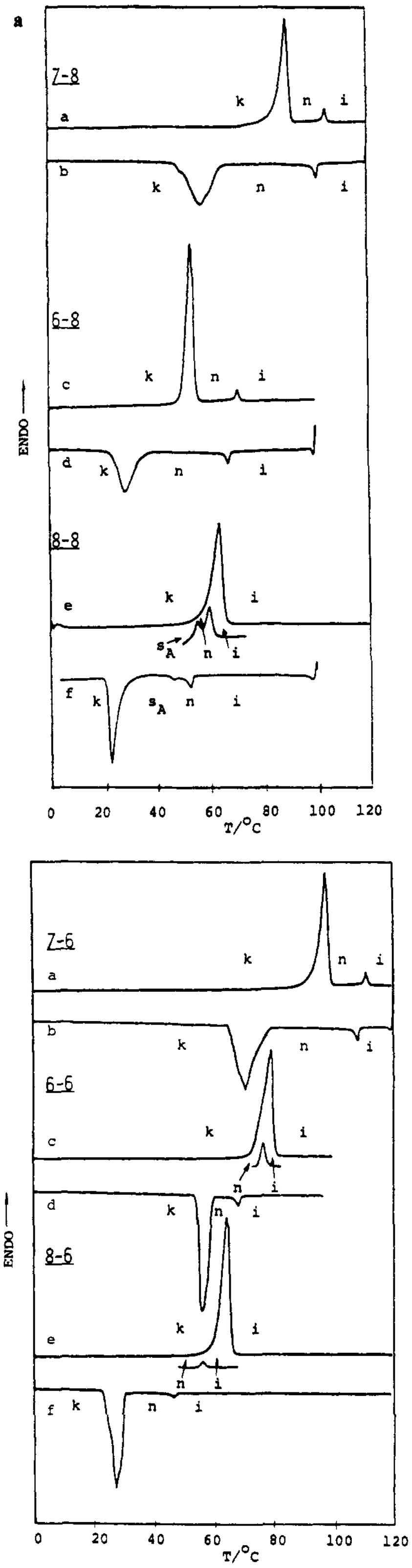

Figure 3. (a) Heating and cooling DSC traces of 7-8 (a, b), 6-8 (c, d), and 8-8 (e, f). (b) Heating and cooling DSC traces of 7-6 (a, b), 6-6 (c, d), and 8-6 (e, f).

represent the models of the monomeric structural units of poly{8-[4(cyano-4′-biphenyl)oxy]octyl vinyl ether} [poly(6-8)] and poly{6-[(4-cyano-4′-biphenyl)oxy]hexyl vinyl ether} [poly(6-6)].

Experimental Section

Materials. 4-Phenylphenol (98%), 1,10-phenanthroline (anhydrous, 99%), palladium(II) acetate (all from Lancaster Synthesis), ferric chloride anhydrous (98%, Fluka), copper(I) cyanide (99%), *n*-butyl vinyl ether (98%), 9-borabicyclo[3.3.1]nonane (9-BBN, crystalline, 98%), 8-bromo-1-octanol (95%), 6-chlorohexan-1-ol (97%), and the other reagents (all from Aldrich) were used as received. Methyl sulfide (anhydrous, 99%, Aldrich) was refluxed over 9-BBN and then distilled under argon. Dichloromethane (99.6%, Aldrich), used as a polymerization solvent, was first washed with concentrated sulfuric acid and then with water, dried over anhydrous magnesium sulfate, refluxed over calcium hydride, and freshly distilled under argon before each use. *N*-Methyl-2-pyrrolidone (98%, Lancaster Synthesis) was dried by azeotropic distillation with benzene, shaken with barium

Table II
Cationic Polymerization of 8-[(4-Cyano-4′-biphenyl)oxy]octyl Vinyl Ether (6-8) (Polymerization Temperature 0 °C; Polymerization Solvent Methylene Chloride; $[M]_0$ = 0.285 M; $[(CH_3)_2S]_0/[I]_0$ = 10; Polymerization Time 1 h) and Characterization of the Resulting Polymers

			GPC			phase transitions, °C (corresponding enthalpy changes, kcal/mru)	
sample	$[M]_0/[I]_0$	polym yield, %	$10^{-3}M_n$	M_w/M_n	DP	heating	cooling
1	2.0	42.3	0.75	1.11	2.2	g −6.4 s_A 65.1 $(-)^a$ n 67.4 $(0.28)^a$ i g −6.7 s_A 63.8 $(-)^4$a n 65.6 $(0.31)^a$ i	i 65.0 $(0.29)^a$ n 63.5 $(-)^a$ s_A −6.4 g
2	4.0	68.0	1.47	1.06	4.2	g 4.9 s_A 110.9 (0.48) i g 2.5 s_A 110.5 (0.47) i	i 105.6 (0.46) s_A 0.1 g
3	6.0	65.0	2.06	1.07	5.9	g 5.8 s_A 114.3 (0.51) i g 4.2 s_A 114.0 (0.51) i	i 109.2 (0.50) s_A 2.5 g
4	8.0	69.0	2.87	1.09	8.2	g 9.2 s_A 125.6 (0.47) i g 7.5 s_A 125.8 (0.47) i	i 120.5 (0.46) s_A 7.5 g
5	10.0	71.0	3.57	1.04	10.2	g 12.6 s_A 127.5 (0.43) i g 8.3 s_A 127.3 (0.43) i	i 122.8 (0.46) s_A 7.8 g
6	13.0	76.0	4.32	1.06	12.4	g 15.7 s_X 36.4 (0.31) s_A 136.4 (0.58) i g 9.2 s_A 134.8 (0.46) i	i 128.8 (0.45) s_A 7.9 g
7	18.0	86.0	6.31	1.11	18.1	g 23.2 s_X 49.4 (0.27) s_A 145.0 (0.50) i g 17.5 s_X 49.1 (0.27) s_A 144.9 (0.44) i	i 139.6 (0.30) s_A 40.9 (0.44) s_X 12.5 g
8	23.0	85.0	7.89	1.09	22.6	g 22.5 s_X 67.1 (0.27) s_A 154.1 (0.48) i g 18.7 s_X 62.1 (0.28) s_A 151.1 (0.43) i	i 141.6 (0.32) s_A 49.7 (0.40) s_X 13.3 g
9	30.0	69.0	10.88	1.11	31.1	g 22.7 s_X 69.0 (0.34) s_A 155.1 (0.41) i g 21.5 s_X 67.9 (0.31) s_A 155.3 (0.40) i	i 150.0 (0.32) s_A 62.8 (0.39) s_X 19.2 g

[a] Overlapped peaks.

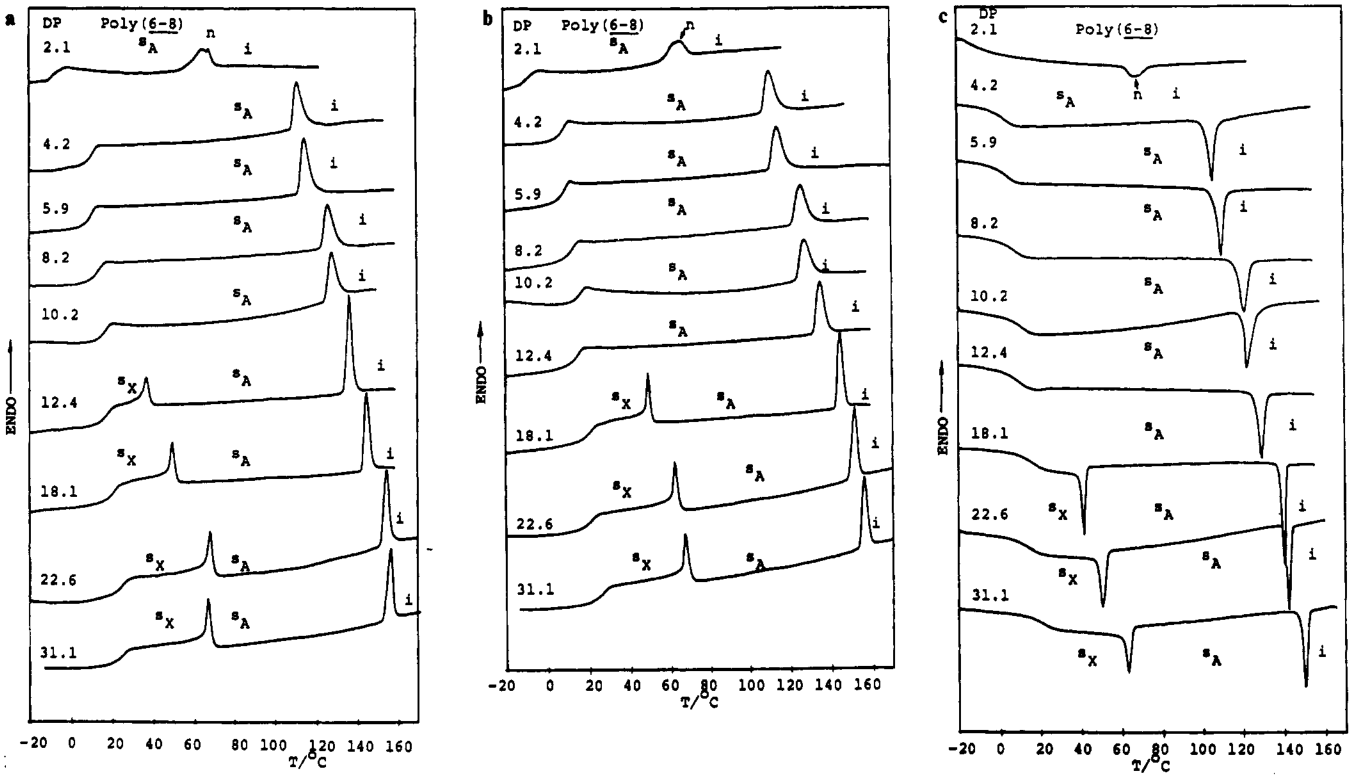

Figure 4. DSC traces displayed during the first heating scan (a), second heating scan (b), and first cooling scan (c) by poly(6-8) with different degrees of polymerization (DP). DP is printed on the top of each DSC scan.

oxide, filtered, and fractionally distilled under reduced pressure. Trifluoromethanesulfonic acid (triflic acid, 98%, Aldrich) was distilled under argon.

Techniques. ^{1}H NMR (200 MHz) spectra were recorded on a Varian XL-200 spectrometer. TMS was used as internal standard. A Perkin-Elmer DSC-4 differential scanning calorimeter, equipped with a TADS 3600 data station, was used to determine the thermal transitions, which were reported as the maxima and minima of their endothermic or exothermic peaks, respectively. In all cases, heating and cooling rates were 20 °C/min unless otherwise specified. Glass transition temperatures (T_g) were read at the middle of the change in the heat capacity. First heating scans differ from second and subsequent heating scans. However, second and subsequent heating scans are identical. The first heating scans can be reobtained after proper annealing of the polymer sample. A Carl-Zeiss optical polarized microscope (Magnification 100×) equipped with a Mettler FP 82 hot stage and a Mettler FP 800 central processor was used to observe the thermal transitions and to analyze the anisotropic textures.[17,18] Molecular weights were determined by gel permeation chromatography (GPC) with a Perkin-Elmer Series 10 LC instrument equipped with LC-100 column oven, LC-600 autosampler, and a Nelson Analytical 900 series integrator data station. The measurements were made at 40 °C using the UV detector. A set of Perkin-Elmer PL gel columns of 10^4 and 500 Å with chloroform as solvent (1 mL/min) and a calibration plot constructed with polystyrene standards was used to determine the molecular weights. High-pressure liquid chromatography experiments were performed with the same instrument.

Synthesis of Monomers. Scheme I outlines the synthesis of monomers and model compounds.

Scheme II
Mechanism of Living Cationic Polymerization

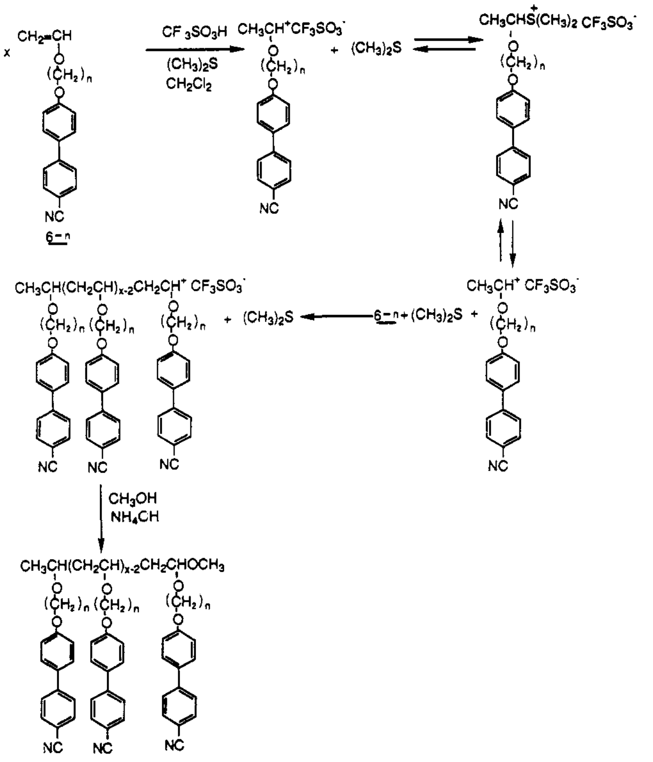

1,10-Phenanthrolinepalladium(II) diacetate (9) was synthesized according to a literature procedure;[19] mp 220 °C. (lit.[19] mp 234 °C).

4-Cyano-4′-hydroxybiphenyl (5) was synthesized as reported in a previous publication;[11] purity 99% (HPLC); mp 195–198 °C (lit.[20,21] mp 196–199 °C). ^{1}H NMR (acetone-d_6, TMS) δ 3.80 (1 proton, OH, s), 7.01 (2 aromatic protons, *o* to –OH, d), 7.61 (2 aromatic protons, *m* to –OH, d), 7.70 (4 aromatic protons, *o* and *m* to –CN, s).

4-Cyano-4′-(8-hydroxyoctan-1-yloxy)biphenyl (7-8): 4-Cyano-4′-hydroxybiphenyl (5.8 g, 0.0297 mol), potassium hydroxide (1.66 g, 0.0297 mol), and few crystals of potassium iodide were dissolved in a mixture of ethanol–water (4/1, 165 mL). 8-Bromo-1-octanol (6.8 g, 0.033 mol) was added to the resulting solution, which was heated to reflux for 24 h. The ethanol was removed on a rotary evaporator, and the resulting solid was washed successively with water, dilute aqueous NaOH, and water. Recrystallization from methanol yielded 5.8 g (60.3%) of white crystals; purity 99.9% (HPLC). ^{1}H NMR ($CDCl_3$, TMS) δ 1.01–1.95 (12 protons, $-(CH_2)_6-$, m), 3.66 (2 protons, $-CH_2OH$, t), 4.01 (2 protons, $PhOCH_2-$, t), 7.01 (2 aromatic protons, *o* to alkoxy, d), 7.66 (4 aromatic protons, *o* and *m* to –CN, d of d). Thermal characterization of 7-8 is reported in Table I.

4-Cyano-4′-(6-hydroxyhexan-1-yloxy)biphenyl (7-6) was prepared by using the same procedure as that detailed for the synthesis of 7-8 except that 8-bromo-1-octanol was replaced with 6-chloro-1-hexanol; yield 70.2%; purity 99.8% (HPLC). ^{1}H NMR ($CDCl_3$, TMS) δ 1.05–1.95 (8 protons, $-(CH_2)_4-$, m), 3.64 (2 protons, $-CH_2OH$, t), 4.00 (2 protons, $PhOCH_2O-$, t), 7.01 (2 aromatic protons, *o* to alkoxy, d), 7.55 (2 aromatic protons, *m* to alkoxy, d), 7.66 (4 aromatic protons, *o* and *m* to –CN, d of d). Thermal transitions of 7-6 are reported in Table I.

8-[(4-Cyano-4′-biphenyl)oxy]octyl vinyl ether (6-8): 7-8 (4.5 g, 0.0139 mmol) was added to a mixture of 1,10-phenanthrolinepalladium(II) diacetate (0.55 g, 1.39 mmol), *n*-butyl vinyl ether (76 mL), and dry chloroform (70 mL). The mixture was heated at 60 °C for 6 h. After cooling and filtration (to remove the catalyst), the solvent was distilled in a rotary evaporator, and the product was purified by column chromatography (silica gel, methylene chloride eluent) to yield 3.4 g (69.9%) of white crystals; purity 99.9% (HPLC). ^{1}H NMR ($CDCl_3$, TMS) δ 1.01–1.95 (12 protons, $-(CH_2)_6-$, m), 3.68 (2 protons, $-CH_2O-$, t), 4.00 (3 protons, $OCH{=}CH_2$, trans, and $PhOCH_2-$, m), 4.14 and 4.21 (1 proton, $-OCH{=}CH_2$, cis, d), 6.49 (1 proton, $-OCH{=}CH_2$, q), 7.01 (2 aromatic protons, *o* to alkoxy, d), 7.50 (2 aromatic protons, *m* to alkoxy, d), 7.66 (4 aromatic protons, *o* and *m* to –CN, d of d). Thermal transitions of 6-8 are reported in Table I.

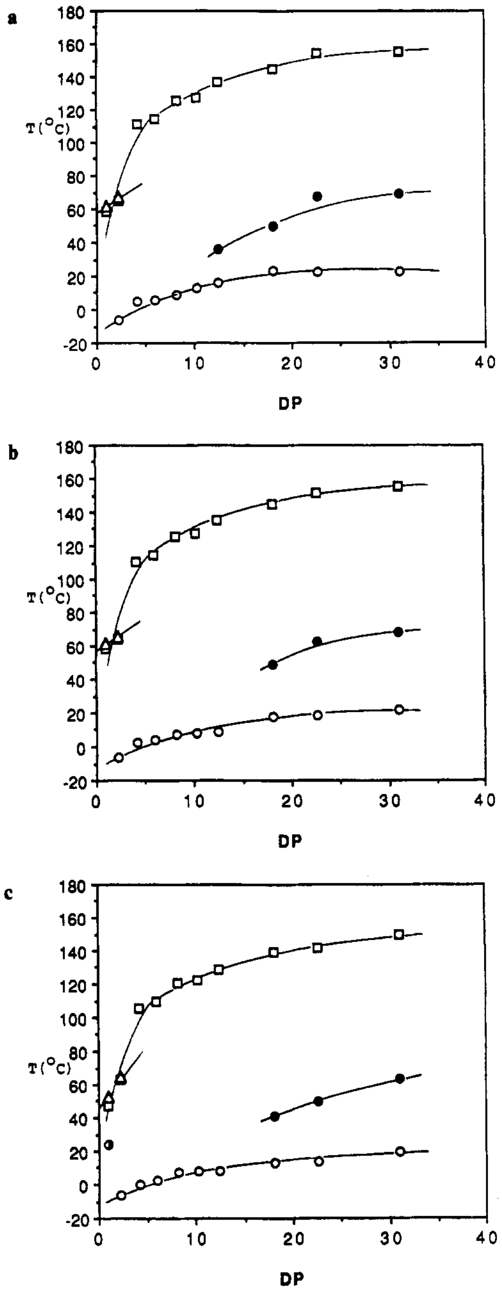

Figure 5. Dependence of phase transition temperatures on the degree of polymerization of poly(6-8). DP = 1 corresponds to 8-8. (a) Data from first heating (fh) scan: ○, T_g (fh); □, T_{s_A-n} or T_{s_A-i} (fh); △, T_{n-i} (fh); ●, $T_{s_X-s_A}$ (fh). (b) Data from second heating (sh) scan: ○, T_g (sh); □, T_{s_A-n} or T_{s_A-i} (sh); △, T_{n-i} (sh); ●, $T_{s_X-s_A}$ (sh). T_m's of 8-8 from first and second heating scans are not plotted. (c) Data from the cooling scan: □, T_{i-s_A}; △, T_{i-n}; ●, $T_{s_A-s_X}$; ○, T_g; ◑, T_k.

6-[(4-Cyano-4′-biphenyl)oxy]hexyl vinyl ether (6-6) was synthesized by the same procedure as for 7-6; yield 85%; purity 99% (HPLC). ^{1}H NMR ($CDCl_3$, TMS) δ 1.01–1.95 (8 protons, $-(CH_2)_4-$, m), 3.70 (2 protons, $-CH_2O-$, t), 4.00 (3 protons, $-OCH{=}CH_2$, trans, and $PhOCH_2-$, m), 4.14 and 4.21 (1 proton, $-OCH{=}CH_2$, cis, d), 6.45 (1 proton, $-OCH{=}CH_2$, q), 7.01 (2 aromatic protons, *o* to alkoxy, d), 7.50 (2 aromatic protons, *m* to alkoxy, d), 7.66 (4 aromatic protons, and aro (4 aromatic protons, and *m* to –CN, d of d). Thermal transitions are reported in Table I.

8-[(4-Cyano-4′-biphenyl)oxy]octyl ethyl ether (8-8): 7-8 (3.23 g, 0.01 mol) was added to a solution containing potassium

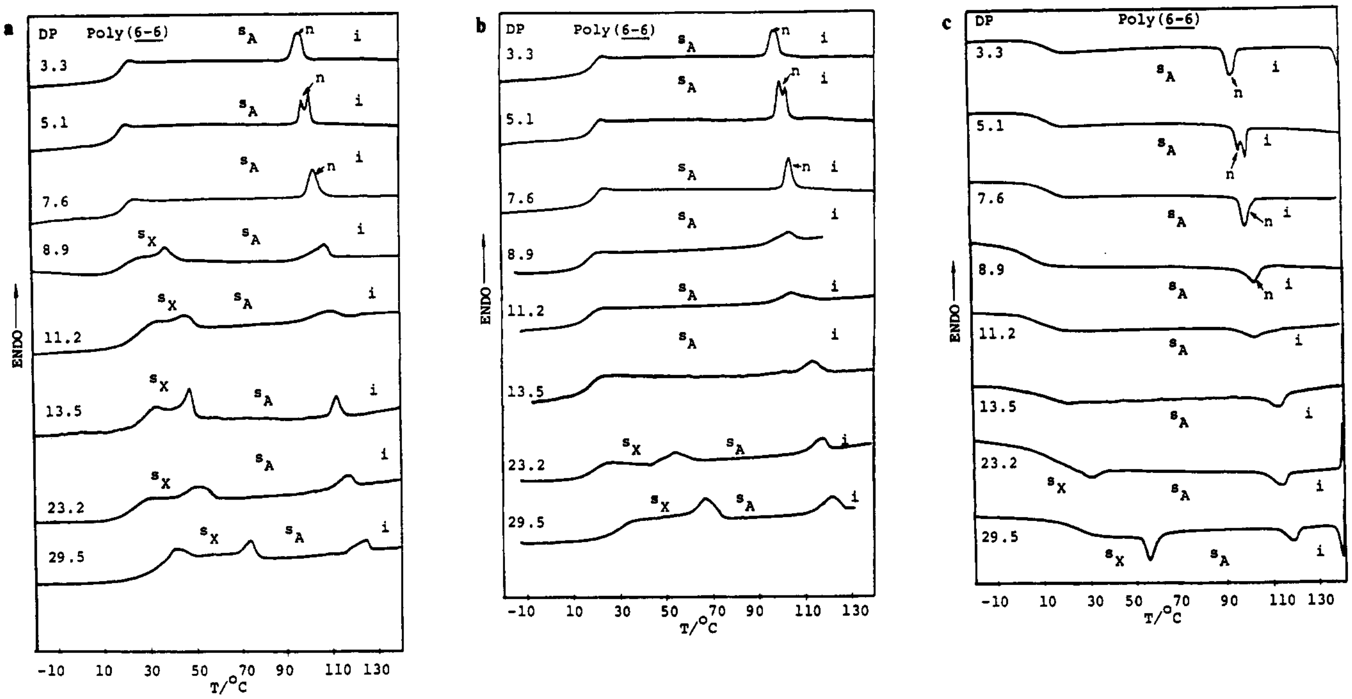

Figure 6. DSC traces displayed during first heating scan (a), second heating scan (b), and first cooling scan (c) by poly(6-6) with different degrees of polymerization (DP). DP is printed on the top of each DSC scan.

Table III
Cationic Polymerization of 6-[(4-Cyano-4′-biphenyl)oxy]hexyl Vinyl Ether (6-6) (Polymerization Temperature 0 °C; Polymerization Solvent Methylene Chloride; $[M]_0$ = 0.311M; $[(CH_3)_2S]_0/[I]_0$ = 10; Polymerization Time 1 h) and Characterization of the Resulting Polymers

			GPC			phase transitions, °C (corresponding enthalpy change, kcal/mru)	
sample	$[M]_0/[I]_0$	polym yield, %	$10^{-3}M_n$	M_w/M_n	DP	heating	cooling
1	4.0	63	1.06	1.02	3.3	g 12.1 s_A 90.8 (–)[a] n 95.7 (0.22)[a] i g 12.1 s_A 91.4 (–)[a] n 95.1 (0.21)[a] i	i 91.5 (0.21)[a] n 86.7 (–)[a] s_A 3.3 g
2	5.0	67	1.65	1.03	5.1	g 16.4 s_A 98.7 (–)[a] n 100.8 (0.28)[a] i g 13.2 s_A 99.2 (–)[a] n 101.2 (0.20)[a] i	i 97.5 (0.20)[a] n 94.8 (–)[a] s_A 7.2 g
3	7.0	76	2.44	1.07	7.6	g 17.9 s_A 101.9 (–)[a] n 102.8 (0.25)[a] i g 16.4 s_A 101.5 (–)[a] n 102.6 (0.19)[a] i	i 100.7 (0.19)[a] n 98.8 (–)[a] s_A 4.8 g
4	9.0	84	2.87	1.03	8.9	g 17.7 s_X 37.3 (0.21) s_A 107.8 (0.17) i g 17.5 s_A 104.0 (0.14) i	i 102.4 (0.19)[a] n 100.8 (–)[a] s_A 4.8 g
5	11.0	72	3.59	1.10	11.2	g 26.2 s_X 45.6 (0.30) s_A 109.1 (0.15) i g 15.6 s_A 104.0 (0.14) i	i 105.0 (0.19) s_A 5.6 g
6	13.0	75	4.33	1.05	13.5	g 28.9 s_X 47.7 (0.45) s_A 112.2 (0.15) i g 15.7 s_A 112.7 (0.21) i	i 111.9 (0.19) s_A 3.7 g
7	23.0	85	7.45	1.09	23.2	g 24.3 s_X 52.0 (0.25) s_A 117.1 (0.15) i g 23.2 s_X 53.9 (0.23) s_A 117.4 (0.14) i	i 113.4 (0.18) s_A 36.2 (0.06) s_X 12.7 g
8	30.0	87	9.47	1.10	29.5	g 28.9 s_X 73.9 (0.32) s_A 124.8 (0.12) i g 29.5 s_X 67.1 (0.46) s_A 120.5 (0.15) i	i 117.6 (0.15) s_A 54.1 (0.29) s_X 25.8 g

[a] Overlapped peaks.

tert-butoxide (1.12 g, 0.01 mol) and 18-crown-6 (2.6 mg, 0.01 mmol) in dry tetrahydrofuran (78 mL). Diethyl sulfate (1.54 g, 0.01 mol) was added, and the reaction mixture was refluxed for 3 h. After cooling, the reaction mixture was extracted with chloroform, washed with water, and dried over magnesium sulfate, and the chloroform was removed in a rotary evaporator. The resulting product was purified by column chromatography (silica gel, methylene chloride eluent) to yield 2.2 g (63%) of white crystals; purity 99.9% (HPLC). ^1H NMR ($CDCl_3$, TMS) δ 1.20 (3 protons, $-OCH_2CH_3$, t), 1.30–1.81 (12 protons, $-(CH_2)_6-$, m), 3.41 (4 protons, $-CH_2OCH_2CH_3$, m), 4.00 (2 protons, $-CH_2OPh$, t), 7.01 (2 aromatic protons, *o* to alkoxy, d), 7.51 (2 aromatic protons, *m* to alkoxy, d), 7.66 (4 aromatic protons, *o* and *m* to –CN, d of d). Thermal transitions of 8-8 are reported in Table I.

6-[(4-Cyano-4′-biphenyl)oxy]hexyl ethyl ether (8-6) was synthesized by the same procedure as for 6-6; yield 67%; purity 99.9% (HPLC). ^1H NMR ($CDCl_3$, TMS) δ 1.21 (3 protons, $-OCH_2CH_3$, t), 1.46–1.82 (8 protons, $-(CH_2)_4-$, m), 3.43 (4 protons, $-CH_2OCH_2CH_3$, m), 4.01 (2 protons, $-CH_2OPh$, t), 7.02 (2 aromtic protons, *o* to alkoxy, d), 7.51 (2 aromatic protons, *m* to alkoxy, d), 7.68 (4 aromatic protons, *o* and *m* to –CN, d of d). Thermal transitions of 8-6 are reported in Table I.

Cationic Polymerizations. Polymerizations were carried out in glass flasks equipped with Teflon stopcocks and rubber septa under argon atmosphere at 0 °C for 1 h. All glassware was dried overnight at 130 °C. The monomer was further dried under vacuum overnight in the polymerization flask. Then the flask was filled with argon and cooled to 0 °C, and the methylene chloride, dimethyl sulfide, and triflic acid were added via a syringe. The monomer concentration was about 10 wt % of the solvent volume, and the dimethyl sulfide concentration was 10 times larger than that of the initiator. The polymer molecular weight was controlled by the monomer/initiator ratio. At the end of the polymerization the reaction mixtures were precipitated into methanol containing a few drops of NH_4OH. The filtered polymers were dried and precipitated from methylene chloride solutions into methanol until GPC traces showed no traces of monomer. Tables II and III summarize the polymerization results. Although the polymer yields are lower than expected due to losses during the purification process, the conversions were almost quantitative in all cases.

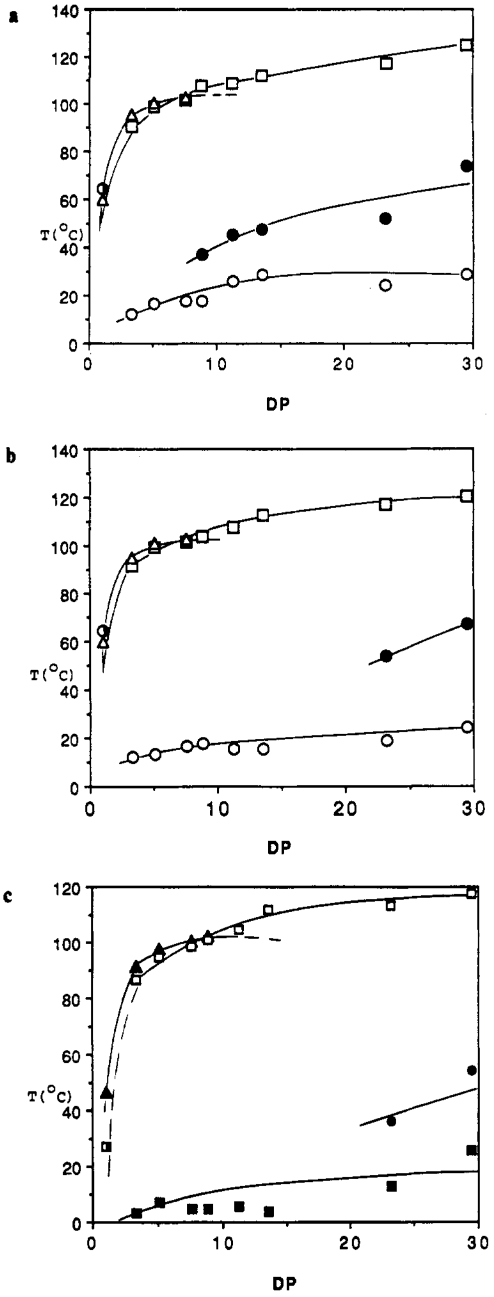

Figure 7. Dependence of the phase-transtion temperatures on the degree of polymerization of poly(6-6). DP = 1 corresponds to 8-6. (a) Data from first heating scan: ○, T_g (fh); □, $T_{s_A\text{-}n}$ (fh) or $T_{s_A\text{-}i}$ (fh); △, $T_{n\text{-}i}$ (fh); ●, $T_{s_X\text{-}s_A}$ (fh); ◑, T_m (fh). (b) Data from second heating scan: ○, T_g (sh); □, $T_{s_A\text{-}n}$ (sh) or $T_{s_A\text{-}i}$ (sh); △, $T_{n\text{-}i}$ (sh); ●, $T_{s_X\text{-}s_A}$ (sh); ◑, T_m (sh). (c) Data from cooling scan: ▲, $T_{i\text{-}n}$; □, $T_{n\text{-}s_A}$ or $T_{i\text{-}s_A}$; ●, $T_{s_A\text{-}s_X}$; ■, T_g; ▣, T_k.

Results and Discussion

The synthesis of 6-8, 6-6, 8-8, and 8-6 are outlined in Scheme I. Although 6-8 and 6-6 can be synthesized by the etherification of 4-cyano-4′-hydroxybiphenyl with 8-bromooctyl vinyl ether and 6-bromohexyl vinyl ether, respectively, as outlined in Scheme I,[8-12,14,23] the preferred route consists of the transetherification of 7-8 and 7-6, respectively, with *n*-butyl vinyl ether. This reaction is catalyzed by 1,10-phenanthrolinepalladium(II) diacetate.[19,22]

As shown previously,[8-10,11,14,15,24-26] living cationic polymerization of vinyl ethers tolerates a variety of functional groups. We prefer to perform this polymerization with triflic acid/dimethyl sulfide initiator, since this polymerization can be carried out in methylene chloride at 0 °C.[11,15,27,28] Scheme II outlines the polymerization mechanism. Under our polymerization conditions, the polyethers contain acetal chain ends (Scheme II), and therefore they should be manipulated in the absence of acids.

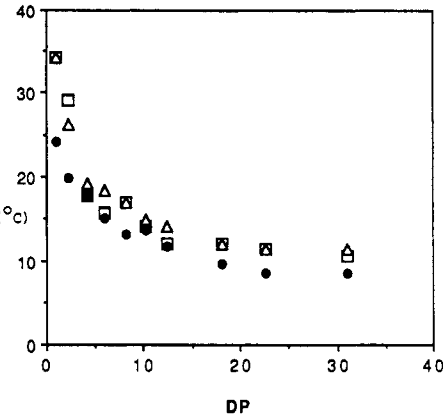

Figure 8. Dependence of the peak width ΔT (°C) of the mesomorphic–isotropic and isotropic–mesomorphic phase transition temperatures versus the degree of polymerization of poly(6-8); □, first heating scan; △, second heating scan; ●, cooling scan.

The polymerization results are presented in Tables II and III. GPC traces of poly(6-8) are exhibited in Figure 1. The molecular weights and the molecular weight distributions of both sets of polymers are presented in Tables II and III. All polymers display a narrow molecular weight distribution. The theoretical {i.e., $[M]_0/[I]_0$} and experimental degrees of polymerization of these polymers agree very well (Tables II and III). The dependences of the number average molecular weight (M_n) and of M_w/M_n versus the ratio between the initial monomer 6-8 and initiator concentration $[M]_0/[I]_0$ are plotted in Figure 2. Both plots demonstrate the living character of these polymerizations. Similar plots for poly(6-6) demonstrate that 6-6 polymerizes also through a living mechanism.

Figure 3a displays the heating and cooling differential scanning calorimetry (DSC) traces of 4-cyano-4′-(8-hydroxyoctan-1-yloxy)biphenyl (7-8), 8-[4-cyano-4′-biphenyloxy]octyl vinyl ether (6-8), and 8-[(4-cyano-4′-biphenyl)oxy]octyl ethyl ether (8-8). 7-8 and 6-8 present an enantiotropic nematic mesophase. The model compound of the monomeric structural unit of poly(6-8), i.e., 8-8, presents a monotropic nematic and a monotropic s_A mesophase. The s_A–nematic and nematic–isotropic transitions from the heating scan of 8-8 were determined by reheating the sample in the DSC instrument from the above the temperature at which this compound crystallizes (Figure 3a). Heating and cooling DSC traces of 7-6, 6-6, and 8-6 are shown in Figure 3b. 7-6 exhibits an enantiotropic nematic mesophase, whereas both 6-6 and 8-6 display a monotropic nematic mesophase. All these thermal transitions and the corresponding enthalpy changes are summarized in Table I.

Figure 4 presents the first heating, the second heating, and the cooling DSC scans of poly(6-8). First and subsequent cooling scans of each polymer are identical. With the exception of the poly(6-8) which has a degree of polymerization equal to 12.4, all other polymers display first and subsequent heating scans that are almost identical. The case of poly(6-8) will be discussed later. Poly(6-8) with a degree of polymerization of 2.1 displays an enantiotropic s_A phase and an enantiotropic nematic phase that are almost overlapped on both their heating (Figure 4a,b) and cooling (Figure 4c) scans. Therefore, this dimer resembles the phase behavior of the model of the monomeric structural unit, 8-8, except that the dimer

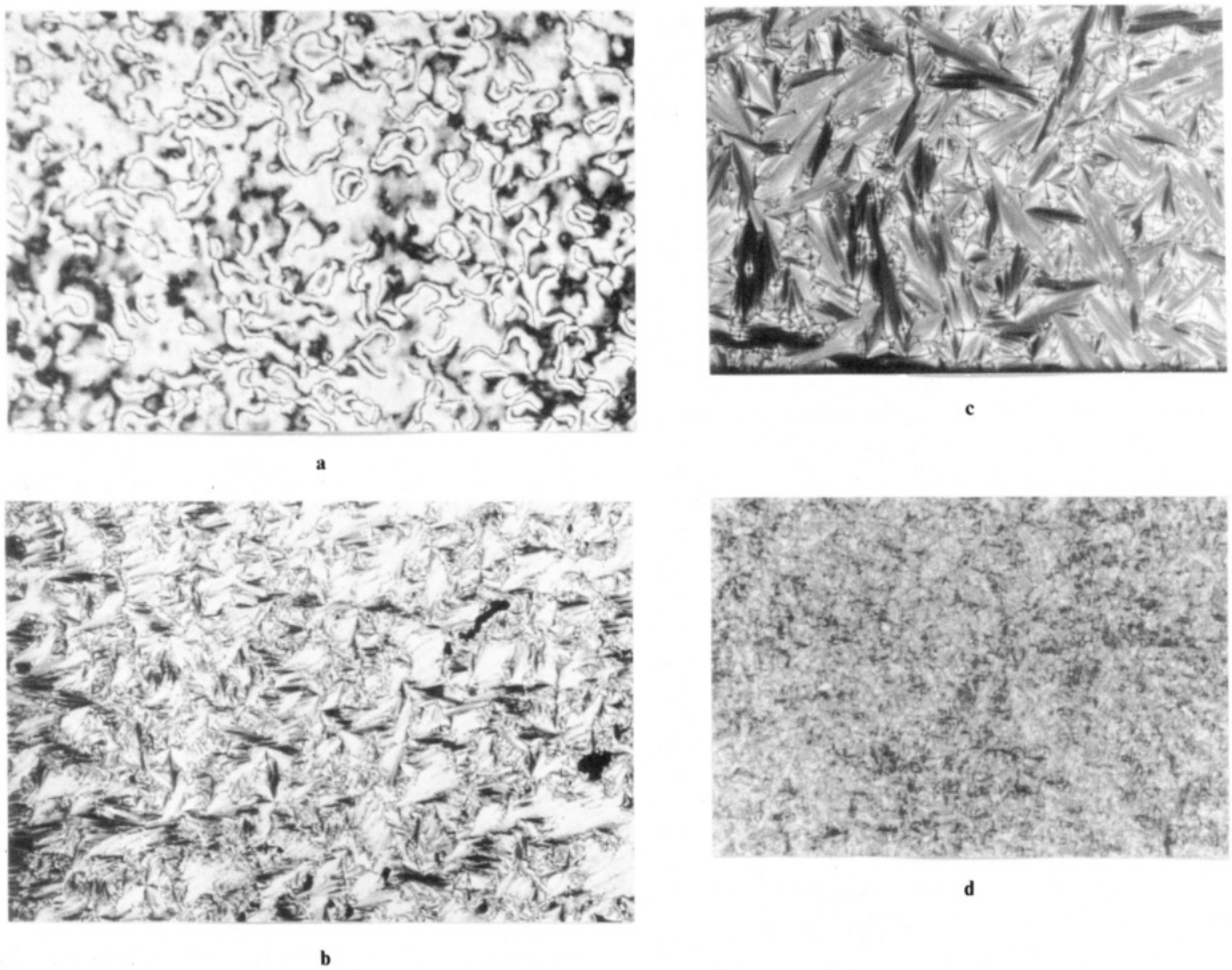

Figure 9. Representative optical polarized micrographs (100×): (a) 8-8 at 53 °C on the cooling scan (nematic phase); (b) 8-8 at 47 °C on the cooling scan (s_A phase); (c) poly(6-8), DP = 31.1 at 150 °C on the cooling scan (s_A phase); (d) poly(6-8), DP = 31.1 at 60 °C on the cooling scan (s_X phase).

does not crystallize and its thermal transitions are shifted toward higher temperatures (Tables I and II). Poly(6-8)s with degrees of polymerization from 4.2 to 10.2 display only an enantiotropic s_A mesophase. Poly(6-8) with degrees of polymerization equal to and higher than 12.4 display a s_X (i.e., a smectic phase that was not yet identified) and an enantiotropic s_A phase. A s_X phase is enantiotropic in the case of polymers with degrees of polymerization from 18.1 to 31.1 and appears only on the first heating scan in the case of the polymers with a degree of polymerization equal to 12.4. This behavior is due to the kinetic effect provided by the close proximity of this phase transition to the glass transition of the polymer.

All these phase-transition temperatures and their corresponding thermodynamic parameters are summarized in Table II.

The thermal transition temperatures from the first heating, second heating, and cooling scans of all polymers are plotted as a function of the degree of polymerization in Figure 5. The phase-transition temperatures of the model compound of the monomeric structural unit (8-8) from Figure 3 and Table I are also included. However, the melting and crystallization temperatures are not plotted since they would overlap the other data. Nevertheless, we have to recall that both the nematic and the s_A phase of 8-8 are monotropic. Figure 5 provides us with the following conclusion. On increasing the degree of polymerization from 1 to 2.1, both the nematic and s_A phase-transition temperatures become enantiotropic. This effect is both due to the decreased rate of crystallization of the dimer, which represents a kinetic effect, and due to the increase of the two phase-transition temperatures with the increase of the molecular weight, which represents a thermodynamic effect. However, on increasing the degree of polymerization from 2.1 to 4.2, the polymer no longer displays the nematic mesophase. Although only from two data points, we can assume that this change represents a continuous dependence of molecular weight. This result is simply due to the fact that the slope of the dependence temperature transition of the s_A phase versus polymerization degree is higher than that of the slope relating the dependence of the nematic temperature transition versus degree of polymerization.

The DSC traces of the first heating, second heating, and cooling scans of poly(6-6) are presented in Figure 6. All cooling scans are identical. The phase-transition temperatures which are not influenced by kinetics are identical on the first, second, and subsequent heating scans. Only phase transitions located in close proximity to the glass transition temperature are dependent on the thermal history of the sample. Poly(6-6)s with degrees of polymerization from 3.3 to 7.6 display enantiotropic s_A and nematic mesophases irrespective of the DSC scan we consider for their characterization (Figure 6). Polymers with degrees of polymerization from 8.9 to 29.5 display an s_X (i.e., an unidentified smectic phase) mesophase in the first heating scan. Only poly(6-6)s with degrees of polymerization from 23.2 to 29.5 display an enantiotropic s_X phase. The s_X phase does not appear on the second heating and cooling scans for polymer samples with degrees of polymerization ranging from 8.9 to 13.5. However, after proper annealing conditions, the s_X mesophase reappears on the first heating scan. That is, for polymer samples with degrees of polymerization from 8.9 to 13.5, under equilibrium conditions the s_X phase is "inverse" monotropic. This behavior demonstrates that mesophases located in close proximity to the glass transition temperature are subjected to strong kinetic influences.

The phase-transition temperatures collected from the first and second heating and the cooling DSC scans are plotted in Figure 7. The phase-transition temperatures of the model compound of the monomeric structural unit (8-6) are also plotted and correspond to a degree of polymerization equal to 1. The plots from Figure 7 demonstrate a clear trend. Both the nematic–isotropic and the s_A–nematic or s_A–isotropic as well as their reversed transition temperatures display continuous dependences of polymerization degree. Let us assume that 8-6 displays a virtual s_A mesophase. Under these conditions, the dependence of nematic–isotropic transition temperature versus polymerization degree has a higher slope than the dependence of the s_A–nematic, s_A–isotropic transition temperatures versus polymerization degree. Above the degree of polymerization where these two dependences intersect each other, the nematic mesophase should appear below the s_A mesophase, and therefore it becomes "virtual". This behavior can explain the change of the highest temperature mesophase from nematic to smectic upon increasing the degree of polymerization.

It is generally accepted that many nematic monomers lead to smectic side-chain liquid-crystalline polymers.[1] However, it is not correct to compare the phase behavior of monomers with that of the corresponding polymers since as observed from Figure 3, small changes in the structure of the monomer change drastically their phase behavior. Most frequently, the mesomorphic behavior of the monomer is different from that of the model compound of the monomeric structural unit.[11] To our knowledge, this is the first time when it is experimentally observed that the change of the mesophase of the monomeric structural unit represents a continuous dependence of molecular weight. Such a dependence was previously demonstrated only for the case of a main-chain liquid-crystalline polymer.[29]

The formation of a second mesophase at higher polymer molecular weights as is the case of the s_X phase from this example was observed previously.[7,11] Such a dependence on polymer molecular weight can be explained by a simple thermodynamic scheme.[12,13] However, an explanation for the transformation of a nematic–isotropic phase into a smectic–isotropic phase by increasing the molecular weight of the polymer should also consider the different degrees of distortion of the random-coil conformation of the polymer backbone in the nematic and smectic mesophase.[1,31-35] This discussion will represent the subject of a further publication.

An additional trend observed in Figure 4 refers to the dependence of the width of the s_A–isotropic and isotropic–s_A phase transition peaks on the polymer molecular weight. This width decreases with the increase of the polymer molecular weight. Figure 8 illustrates this trend. A similar trend was observed for two other polymers based on flexible backbones and displaying a smectic–isotropic transition.[6,11] An explanation for this behavior was provided in a previous publication.[6]

Figure 9 presents some representative textures displayed by the nematic, s_A, and s_X phases exhibited by 8-8 (degree of polymerization of 1) and poly(6-8) with a degree of polymerization of 31.1. The nematic and s_A mesophases of poly(6-8) with a degree of polymerization of 2.1 exhibit the same textures as those of 8-8.

Acknowledgment. Financial support from the Office of Naval Research is gratefully acknowledged.

References and Notes

(1) Percec, V.; Pugh, C. In *Side Chain Liquid Crystal Polymers*; McArdle, C. B., Ed.; Chapman and Hall: New York, 1989; p 30 and references therein.
(2) Kostromin, S. G.; Talroze, R. V.; Shibaev, V. P.; Plate, N. A. *Makromol. Chem. Rapid Commun.* **1982**, *3*, 803.
(3) Stevens, H.; Rehage, G.; Finkelmann, H. *Macromolecules* **1984**, *17*, 851.
(4) Shibaev, V. *Mol. Cryst. Liq. Cryst.* **1988**, *155*, 189.
(5) Uchida, S.; Morita, K.; Miyoshi, K.; Hashimoto, K.; Kawasaki, K. *Mol. Cryst. Liq. Cryst.* **1988**, *155*, 93.
(6) Percec, V.; Hahn, B. *Macromolecules* **1989**, *22*, 1588.
(7) Percec, V.; Tomazos, D.; Pugh, C. *Macromolecules* **1989**, *22*, 3259.
(8) Sagane, T.; Lenz, R. W. *Polym. J.* **1988**, *20*, 923.
(9) Sagane, T.; Lenz, R. W. *Polymer* **1989**, *30*, 2269.
(10) Sagane, T.; Lenz, R. W. *Macromolecules* **1989**, *22*, 3763.
(11) Percec, V.; Lee, M.; Jonsson, H. *J. Polym. Sci., Part A: Polym. Chem.*, in press.
(12) Percec, V.; Keller, A. *Macromolecules* **1990**, *23*, 4347.
(13) Keller, A.; Ungar, G.; Percec, V. In *Advances in Liquid Crystalline Polymers*; Ober, C. K., Weiss, R. A., Eds., ACS Symposium Series 435; American Chemical Society: Washington, DC, 1990; p 308.
(14) Rodriguez-Parada, J. M.; Percec, V. *J. Polym. Sci., Part A: Polym. Chem.* **1986**, *24*, 1363.
(15) Rodenhouse, R.; Percec, V.; Feiring, A. E. *J. Polym. Sci., Part C: Polym. Lett.* **1990**, *28*, 345.
(16) Adams, J.; Gronski, W. *Makromol. Chem. Rapid Commun.* **1989**, *10*, 553.
(17) Demus, D.; Richter, L. *Textures of Liquid Crystals*; Verlag Chemie: Weinheim, FRG, 1978.
(18) Gray, G. W.; Goodby, J. W. *Smectic Liquid Crystals. Textures and Structures*; Leonard Hill: Glasgow, 1984.
(19) McKeon, J. E.; Fitton, P. *Tetrahedron* **1972**, *28*, 223.
(20) Hsu, C. S.; Rodriguez-Parada, J. M.; Percec, V. *J. Polym. Sci., Part A: Polym. Chem.* **1987**, *25*, 2425.
(21) Gray, G. W.; Harrison, H. J.; Nash, J. A.; Constant, J.; Hulme, D. S.; Kirton, J.; Raynes, E. P. In *Ordered Fluids and Liquids Crystals*; Porter, R. S., Johnson, J. F., Eds.; Plenum: New York, 1974; Vol. II, p 617.
(22) McKeon, J. E.; Fitton, P.; Griswold, A. A. *Tetrahedron* **1972**, *28*, 227.
(23) Percec, V.; Tomazos, D. *Polym. Bull.* **1987**, *18*, 239.
(24) Higashimura, T.; Aoshima, S.; Sawamoto, M. *Makromol. Chem. Macromol. Symp.* **1988**, *13/14*, 457.
(25) Sawamoto, M.; Aoshima, S.; Higashimura, M. *Makromol. Chem. Macromol. Symp.* **1988**, *13/14*, 513.
(26) Higashimura, T.; Sawamoto, M. In *Comprehensive Polymer Science*; Allen, G., Bevington, J., Eds.; Pergamon Press: Oxford, 1989; Vol. 3, p 684.
(27) Feit, B. A.; Cho, C. G.; Webster, O. W. In *9th International Symposium on Cationic Polymerization and Related Ionic Processes*; Strasbourg, June 5–9, 1989; Abstracts, p 59.
(28) Lin, C. H.; Matyjaszewski, K. *Polym. Prepr. (Am. Chem. Soc., Div. Polym. Chem.)* **1990**, *31/1* 599.
(29) Kumar, R. S.; Clough, S. B.; Blumstein, A. *Mol. Cryst. Liq. Cryst.* **1988**, *157*, 387.
(30) Percec, V., Lee, M., to be published.
(31) Warner, M. In *Side Chain Liquid Crystal Polymers*; McArdle, C. B., Ed.; Chapman and Hall: New York, 1989; p 7 and references therein.
(32) Noel, C. In *Side Chain Liquid Crystal Polymers*; McArdle, C. B., Ed.; Chapman and Hall: New York, 1989; p 159.
(33) Pepy, G.; Cotto, J. P.; Hardouin, F.; Keller, P.; Lambert, M.; Mousa, F.; Noirez, L.; Lapp, A.; Strazzielle, C. *Makromol. Chem. Macromol. Symp.* **1988**, *15*, 251.
(34) Percec, V.; Tomazos, D. *Polymer* **1990**, *31*, 1658.
(35) Percec, V.; Hahn, B.; Ebbert, M.; Wendorff, J. H. *Macromolecules* **1990**, *23*, 2092.